Fair sampling perspective on an apparent violation of duality

Eliot Bolduc[a,b,1], Jonathan Leach[b], Filippo M. Miatto[a], Gerd Leuchs[a,c,d], and Robert W. Boyd[a,e,f]

[a]Department of Physics, University of Ottawa, Ottawa, ON, Canada K1N 6N5; [b]School of Engineering and Physical Sciences, Heriot-Watt University, Edinburgh EH14 4AS, United Kingdom; [c]Institute of Optics, Information and Photonics, University of Erlangen-Nuremberg, 91058 Erlangen, Germany; [d]Max Planck Institute for the Science of Light, 91058 Erlangen, Germany; [e]Institute of Optics, University of Rochester, Rochester, NY 14627; and [f]School of Physics and Astronomy, University of Glasgow, Glasgow G12 8QQ, United Kingdom

Edited by Peter J. Rossky, The University of Texas at Austin, Austin, TX, and approved July 15, 2014 (received for review January 16, 2014)

In the event in which a quantum mechanical particle can pass from an initial state to a final state along two possible paths, the duality principle states that "the simultaneous observation of wave and particle behavior is prohibited" [Scully MO, Englert B-G, Walther H (1991) *Nature* 351:111–116]. Whereas wave behavior is associated with the observation of interference fringes, particle behavior generally corresponds to the acquisition of which-path information by means of coupling the paths to a measuring device or part of their environment. In this paper, we show how the consequences of duality change when allowing for biased sampling, that is, postselected measurements on specific degrees of freedom of the environment of the two-path state. Our work gives insight into a possible mechanism for obtaining simultaneous high which-path information and high-visibility fringes in a single experiment. Further, our results introduce previously unidentified avenues for experimental tests of duality.

wave-particle complementarity | double-slit experiment | decoherence

In his famous analysis of the two-slit experiment, Bohr arrived at the conclusion that one cannot obtain both complete which-way information and interference effects in a single experimental configuration (1). Since then, numerous studies have reinforced and refined Bohr's result (2–7). Further, the duality principle was confirmed by experimental evidence with photons (8) and massive particles such as neutrons (3) and atoms (9). Having passed every test to date, duality has indubitably become a solid and universal principle of quantum mechanics.

Recently, however, Menzel et al. reported a surprising result in the context of the duality principle (10, 11). They implemented Young's two-slit experiment with photons entangled in position and momentum generated through spontaneous parametric down-conversion (SPDC) and measured both an interference pattern with high visibility and high which-way information in a single experimental configuration. Motivated by this unexpected result, we analyze duality from a "fair sampling" perspective.

The concept of fair sampling has received much attention in the context of tests of the Bell inequalities and nonlocality (12–14). To rule out local theories completely, one should avoid any assumption, including the fair-sampling assumption, which states that the set of measurement results is representative of the entire ensemble under study. To achieve freedom from this assumption one should make sure that the detection efficiency be equal for all of the states in the ensemble and that the overall detection efficiency be above a particular threshold (14), which depends on the type of Bell inequality. Fair sampling also implies that all measurement settings be chosen without bias. In other words, all relevant subsets of an ensemble must be sampled with equal probability. However, the result of a test of fundamental quantum mechanics performed with biased sampling can still bear meaning if all of the properties of the measurement settings are taken into account.

In this work, we derive a tight relation between which-alternative knowledge and average visibility of the corresponding interference pattern in the presence of an environment, an improvement on the bound of the known inequalities. We then show how biased sampling can cause an apparent violation of the duality principle. We finally study the effect of biased sampling on actual tests of the duality principle by applying our duality relation to a model that captures the essence of the work of Menzel et al. (10, 11).

The Duality Relations

A duality relation bounds the visibility of an interference pattern and the corresponding available which-alternative information in an interferometer. Young's two-slit experiment is one of many ways to produce the experimental conditions in which an interference pattern and which-way knowledge can be obtained. Here, we restrict ourselves to a two-alternative system, where the alternatives can correspond to any degree of freedom: the arms of an interferometer, two slits, orthogonal polarizations, and two orbital angular momentum states, to give a few examples. Without specifying any specific degree of freedom, we consider a pure normalized two-alternative quantum state of the form $|\psi\rangle = \lambda_1|1\rangle + \lambda_2|2\rangle$, where λ_1 and λ_2 are the complex amplitudes of alternatives 1 and 2.

There are two distinct ways of gaining which-alternative information: by prediction and by "retrodiction," an educated guess about the outcome of an event that occurred in the past. We review the former and then derive a previously unidentified duality relation for the latter. One can predict, although not necessarily with certainty of being correct, the outcome of a which-alternative measurement if a state is prepared such that a particular alternative is more likely than the other. Greenberger and Yasin, in ref. 3, quantify this fraction with the positive difference between the probabilities of observing the alternatives, $\mathcal{P} = \left||\lambda_1|^2 - |\lambda_2|^2\right|$,

Significance

In 2012, Menzel et al. reported on the results of a fundamental experiment raising questions regarding the simultaneous observation of wave-like and particle-like properties in a given quantum system. Whereas the general applicability of the duality principle to entangled subsystems is an open question, we bring the current understanding of the duality principle a step forward by theoretically deriving the strongest relations between the visibility of an interference pattern and the which-way information in a two-way interferometer such as Young's double slit. This formalism successfully describes tests of duality where postselection on a subset of the interference pattern is applied. Our analysis even reconciles the surprising results of Menzel et al. with the duality principle in its standard form.

Author contributions: E.B., J.L., and R.W.B. designed research; E.B. and J.L. performed research; E.B. and F.M.M. contributed new reagents/analytic tools; E.B. analyzed data; and E.B., J.L., F.M.M., G.L., and R.W.B. wrote the paper.

The authors declare no conflict of interest.

This article is a PNAS Direct Submission.

[1]To whom correspondence should be addressed. Email: eliot.bolduc@gmail.com.

This article contains supporting information online at www.pnas.org/lookup/suppl/doi:10.1073/pnas.1400106111/-/DCSupplemental.

a quantity now known as predictability. It corresponds to one's ability to predict the outcome of a which-alternative measurement in the basis $\{|1\rangle, |2\rangle\}$. The fact that only one outcome is possible for any measurement is usually interpreted as particle-like behavior. The complementary quantity that brings to light the wave-like behavior of the quantum state is the contrast, or visibility, of the interference pattern. The visibility is obtained by projecting $|\psi\rangle$ onto the superposition state $(|1\rangle + e^{i\phi}|2\rangle)/\sqrt{2}$, where ϕ is a phase that is scanned to produce the interference pattern. The visibility of the resulting interference pattern is given by $\mathcal{V} = 2|\lambda_1\lambda_2|$. For a pure two-alternative state, we have the equality

$$\mathcal{P}^2 + \mathcal{V}^2 = 1, \qquad [1]$$

as in ref. 3. In the presence of noise or a statistical mixture of two alternatives, the coherence is reduced and the above relation becomes an inequality: $\mathcal{P}^2 + \mathcal{V}^2 \leq 1$.

The presence of decoherence can be modeled very effectively by considering an auxiliary system (5), often called the environment (6), in addition to the two-alternative system. If the two-alternative system is coupled to an environment, the latter may carry information about the former, and the amount of which-alternative information carried by the environment depends on the strength of the coupling. This concept is concisely explained through an example. Notably, Schwindt et al. have experimentally coupled each path of a Mach–Zehnder interferometer to arbitrary polarization states, making the which-way information accessible through a measurement of the polarization (8). In this experiment, the arms of the Mach–Zehnder interferometer played the role of the two alternatives and the polarization degree of freedom played the role of the auxiliary system. If polarizations of the light in the two paths are orthogonal, a measurement of the polarization of a photon at the output of the interferometer yields complete which-alternative information by retrodiction. The term retrodiction refers to the fact that the measurement outcome, which is obtained after a photon traversed the interferometer, contains the relevant information. Note that for each possible outcome of a measurement on the auxiliary system there corresponds a conditional state of the two-alternative system that will display a particular predictability and a particular visibility; see figure 1 of ref. 7 for a pictorial description.

In an arbitrary basis $\{|a_i\rangle\}$ of dimension D for the auxiliary system, the composite state is written $|\Psi\rangle = \sum_{i=1}^{D} \alpha_i |\psi_i, a_i\rangle$, where the complex amplitudes α_i are normalized $(\sum_i |\alpha_i|^2 = 1)$ and $|\psi_i\rangle = \lambda_{1,i}|1\rangle + \lambda_{2,i}|2\rangle$ are the conditional states. The which-alternative knowledge associated with the composite system is given by the statistical average of the predictabilities, after sorting the auxiliary states $|a_i\rangle$: $\overline{\mathcal{P}} = \sum_i |\alpha_i|^2 \mathcal{P}_i$, where $|\alpha_i|^2$ is the probability of occurrence of the ith auxiliary state and $\mathcal{P}_i$ is the predictability associated with this same auxiliary state $|a_i\rangle$. Because which-alternative knowledge generally depends on the basis chosen to sort the states of the environment, in ref. 7, this quantity $\overline{\mathcal{P}}$ is denoted by $K(O_E)$, where O_E specifies the basis in question. Similarly, the average visibility $\overline{\mathcal{V}}$ is written $\mathcal{V}^{QE}(O_E)$ in ref. 7.

The quantities $\overline{\mathcal{P}^2} = \sum_i |\alpha_i|^2 \mathcal{P}_i^2$ and $\overline{\mathcal{V}^2} = \sum_i |\alpha_i|^2 \mathcal{V}_i^2$ sum to unity, in virtue of Eq. **1**,

$$\overline{\mathcal{P}^2} + \overline{\mathcal{V}^2} = 1. \qquad [2]$$

In the case where the auxiliary system is parameterized by a continuous variable, the sums are replaced by integrals.

To find an equality for the physically relevant quantities, the which-alternative knowledge and the average visibility, we use the variances of each distribution: $\sigma_{\mathcal{P}}^2 = \sum_{i=1}^{D} |\alpha_i|^2 (\mathcal{P}_i - \overline{\mathcal{P}})^2$ and $\sigma_{\mathcal{V}}^2 = \sum_{i=1}^{D} |\alpha_i|^2 (\mathcal{V}_i - \overline{\mathcal{V}})^2$. From Eq. **2** and the identities $\sigma_{\mathcal{P}}^2 = \overline{\mathcal{P}^2} - \overline{\mathcal{P}}^2$ and $\sigma_{\mathcal{V}}^2 = \overline{\mathcal{V}^2} - \overline{\mathcal{V}}^2$, it follows that

$$\overline{\mathcal{P}}^2 + \overline{\mathcal{V}}^2 = 1 - \sigma_{\mathcal{P}}^2 - \sigma_{\mathcal{V}}^2. \qquad [3]$$

Because predictability and visibility are bounded between 0 and 1, each variance can take a maximum value of 1/4. The right-hand side (RHS) of Eq. **3** is thus inherently greater than or equal to 1/2. In the presence of noise or uncontrolled coupling to the environment, the equality becomes an inequality, $\overline{\mathcal{P}}^2 + \overline{\mathcal{V}}^2 \leq 1 - \sigma_{\mathcal{P}}^2 - \sigma_{\mathcal{V}}^2$, where the RHS bounds the left-hand side (LHS) in the tightest way possible. The above bound is consistent with the inequality $K(O_E)^2 + V^{(QE)}(O_E)^2 \leq 1$ from ref. 7.

Eq. **3** holds only when all states of the environment $\{|a_i\rangle\}$ are sampled with equal probability, that is, under the fair-sampling assumption. Because the environment is composed of D states, the sampling probability for any state $|a_i\rangle$ should be $1/D$. When this no longer holds true, the statistics do not reflect the state at hand and the RHS of Eq. **3** no longer bounds the LHS. In particular, this occurs when selecting only a subset of the auxiliary system while rejecting the rest. For instance, one could measure only the subset of the environment corresponding to the highest predictability $\mathcal{P}_{\max}$ and also only the one corresponding to the highest visibility $\mathcal{V}_{\max}$. In general, these subsets are different states of the environment, $|a_j\rangle$ and $|a_k\rangle$ with $j \neq k$. For nonzero variances, the maximum value in each distribution is greater than its respective average value: $\mathcal{P}_{\max} > \overline{\mathcal{P}}$ and $\mathcal{V}_{\max} > \overline{\mathcal{V}}$. Because the quantity $(\mathcal{P}_{\max}^2 + \mathcal{V}_{\max}^2)$ can in principle approach 2, it is possible to observe both high predictability and high visibility in a single experiment. This can appear to be a violation of the duality principle, but it is simply a consequence of the different samplings in the measurements of which-alternative information and visibility.

An Example of an Apparent Violation of Duality

Through a model inspired by the work of Menzel et al. (10, 11), we show the details of how to achieve an apparent violation of duality. Fig. 1 illustrates the precise experiment that we model. We start from a two-photon state composed of signal and idler photons generated through spontaneous parametric down-conversion. A measurement of the idler photon heralds the presence of the signal photon, which traverses a two-slit mask. While the measurement of the position of the idler photons provides which-slit information, the

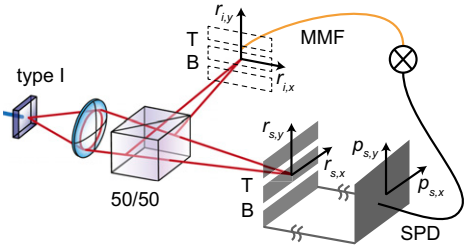

Fig. 1. A model that captures the essence of the experiment of Menzel et al. (10, 11). Photon pairs entangled in position and momentum are generated through degenerate SPDC with a type I crystal and a wide Gaussian pump mode. The signal and idler photons are separated by a 50/50 beam splitter. On the path of the signal photon, the plane of the crystal is imaged with unit magnification to the plane of a two-slit mask made of slit T at $r_{s,y} = d/2$ and slit B at $r_{s,y} = -d/2$. The signal photon traverses the mask, and the idler photon is collected by an optical fiber (MMF), whose input facet is in the image plane of the crystal and centered at $r_{i,y} = d/2$ and $r_{i,x} = 0$. Through position correlations, we gain which-slit information of the signal photon upon detection of the idler photon. We collect the signal photons in the far field of the mask with a scanning point detector (SPD). All measurements are performed in coincidence, such that the interference pattern of the signal photons is conditioned on the detection of idler photons. In a real experiment, interference filters would be placed before the detectors to ensure degenerate SPDC.

heralded signal photons build an interference pattern in the far field of the mask. We give the mathematical details of our model in *Materials and Methods*, where we calculate the quantities appearing in Eq. **3** for a given set of experimental parameters.

The most important result is that the full 2D interference pattern is not uniform. The visibility of the fringes changes as a function of one of the transverse degrees of freedom. In some cases, the maximum visibility significantly surpasses the mean visibility of the full distribution, and this is the requirement to clearly observe an apparent violation of duality.

Results of Our Model. Because of momentum conservation, two photons generated through degenerate SPDC exit the source in opposite transverse directions, ultimately forming a Gaussian-like or a ring-shaped distribution in the far field of the crystal, depending on the value of the phase mismatch parameter φ. In practice this parameter can be adjusted through the angle of the crystal or its temperature; the collinear photon regime resulting in a Gaussian-like far-field distribution corresponds to $\varphi = 0$ rad. Fig. 2 shows the interference patterns formed by the heralded signal photons for a set of phase mismatch parameters. The details of the calculation are shown in *Materials and Methods*; the notation $\tilde{P}_W(\mathbf{p_s}|f_i)$ is from this section and should read "two-dimensional probability density of the signal photon in the far field of the two-slit mask conditioned on the idler photon being coupled to the multimode fiber"; the quantity is not normalized in Fig. 2.

The fact that a ring is not a separable function in its two transverse components plays a key role in our demonstration. For $\varphi = 0$ rad, as in Fig. 2*A*, the mode function takes a Gaussian-like form. Because a 2D Gaussian distribution is separable, the Gaussian-like mode function does not allow the visibility of the fringes to vary significantly as a function of $p_{s,x}$, the horizontal component of the signal photon wavevector that plays the role of a sorted environment. Fig. 2 *B* and *C* shows that the ring opens up as φ becomes more negative, thus allowing for greater variations of the visibility as a function of $p_{s,x}$. The highest-visibility fringes appear where the initial transverse momentum spread $\Delta p_{s,y}$ is narrowest. The maximum visibility is highlighted by dashed lines near position $p_{s,x} = 0$ in Fig. 2*C*. Further, Fig. 2*D* shows the impact of using a Hermite-Gauss 01 (HG_{01}) pump mode on the interference pattern. Given a constant phase mismatch, the visibility of the interference pattern is lower for the HG_{01} pump mode because of the characteristic intensity dip of such a mode. Upon detection of an idler photon on the top slit, the conditioned mode function of the signal photon vanishes at the position of the bottom slit because of this intensity dip in the HG_{01} pump mode. As a consequence, the use of an HG_{01} pump mode increases which-way information at the expense of a lower visibility of the interference pattern. Refs. 10 and 11 analyze the role that the HG_{01} pump mode has in this particular test of complementarity. Specifically, they consider correlations and fringe visibility arising from radiation generated by different sets of atoms inside a nonlinear crystal. Although counterintuitive, they show that the combination of the HG_{01} pump mode and the radiation pattern can lead to high-predictability and high-visibility measurements. In contrast, our alternative and independent explanation does not require the use of an HG_{01} pump mode.

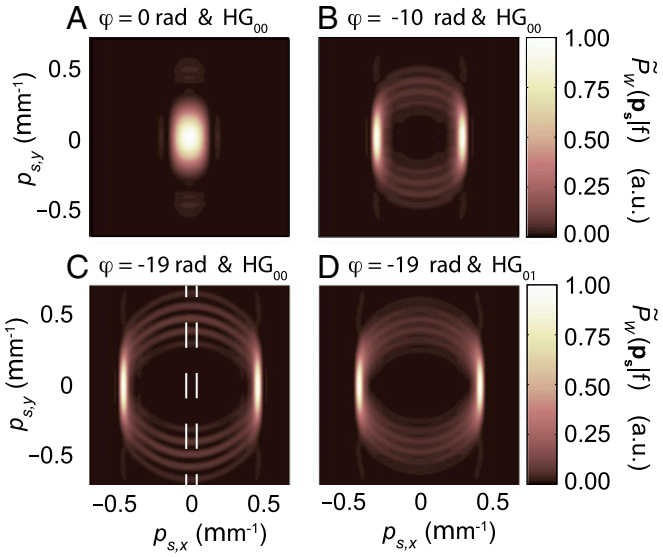

Fig. 2. Conditional interference patterns. *A–D* correspond to various phase mismatch parameters ($\varphi = \{0, -10, -19\}$ rad) and two different pump modes (HG_{00} and HG_{01}). The dashed lines in *C* indicate the state of the environment $p_{s,x} = 0$ corresponding to the highest visibility, which leads to an apparent violation of Eq. **3** when postselected. Whereas the number of fringes is odd on one side of the ring for an HG_{00} pump (*B* and *C*), this number is even for the HG_{01} pump mode (*D*).

To calculate the which-slit information, we compute the distribution issued from the single-slit mask of the top slit and the distribution issued from the single-slit mask of the bottom slit. Again, these distributions are conditioned on the detection of an idler photon incident on the top slit. We explain the complete theoretical procedure in *Materials and Methods* and illustrate the probability distributions issued from the single slits in *Details of Our Numerical Calculations*. The predictability $\mathcal{P}$ is given by the absolute value of the difference between the distribution obtained by blocking the top slit and that obtained by blocking the bottom slit. Fig. 3 shows the probability density $|\alpha_i|^2$ of finding a signal photon at $p_{s,x}$, the predictability $\mathcal{P}$, and the visibility $\mathcal{V}$ as a function of the environment degree of freedom, $p_{s,x}$. For the case of a Gaussian pump (Fig. 3*A*), the relevant parameters amount to $\{\overline{\mathcal{P}} = 0.816, \overline{\mathcal{V}} = 0.331, \mathcal{V}_{\max} = 0.982, \sigma^2_{\mathcal{P}} = 0.077, \sigma^2_{\mathcal{V}} = 0.148\}$. For the case of an HG_{01} pump mode (Fig. 3*B*), the quantities are $\{\overline{\mathcal{P}} = 0.974, \overline{\mathcal{V}} = 0.1538, \mathcal{V}_{\max} = 0.477, \sigma^2_{\mathcal{P}} = 0.0015, \sigma^2_{\mathcal{V}} = 0.0253\}$. In the two cases, Eq. **3** is verified. However, if we calculate what we call the "biased sampling quantity" $\mathcal{B} = \overline{\mathcal{P}}^2 + \mathcal{V}^2_{\max}$, we find a value of $\mathcal{B}_{00} = 1.63$ in the case of a Gaussian pump mode and $\mathcal{B}_{01} = 1.18$ in the case of an HG_{01} pump mode. In both cases, the biased sampling quantity is higher than the ultimate limit of 1 that is normally allowed by duality. Although this result is not a violation of duality, it provides insight into the possibility to record high-visibility fringes while the average predictability is close to unity. A small subset of the photons produces high-visibility fringes, but for this particular subset, however, the predictability is lower than the average predictability of the whole set.

Discussion

The visibility of the interference pattern can be strongly dependent on the state of the degree of freedom of the environment. This is the case in the experiment of Menzel et al. (10, 11), who used entangled particles to perform an elegant test of complementarity. However, entanglement is not a requirement for testing our Eq. **3**. In fact, one could produce similar results without multiparticle entanglement provided that the input mode function is not separable in its horizontal and vertical degrees of freedom. This is closely related to the ongoing discussion on nonseparable mode functions (15, 16).

As a result of this apparent violation one might raise the question of whether this implies a violation of the maximum speed for information transfer being the speed of light. The answer is that it does not and it can be justified in general terms. Our current understanding of quantum physics implies that any measurement on a subsystem that is part of a larger system is perfectly described by the reduced density matrix of the subsystem, which one obtains by tracing over the remaining part of the total quantum system. In the case of entanglement between the subsystem and the remainder

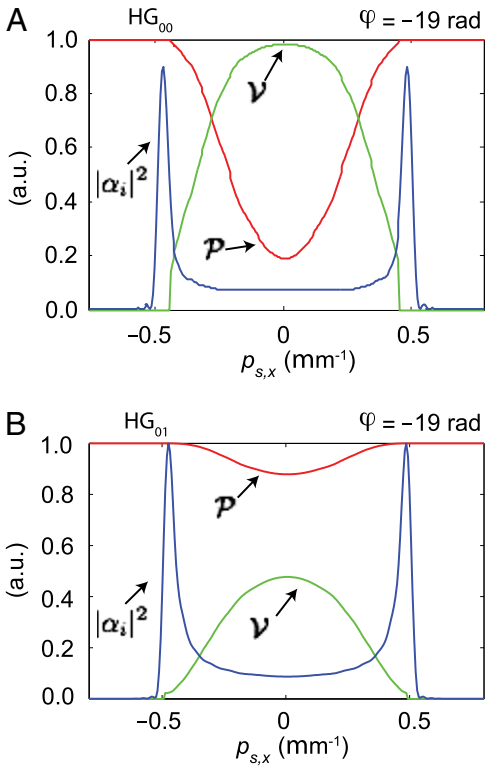

Fig. 3. (*A* and *B*) Plots of the distributions required to calculate the quantities in Eq. **3**. The horizontal axis corresponds to the sorted environment. At all values of $p_{s,x}$, the predictability (red) and the visibility (green) satisfy the equation $\mathcal{P}^2+\mathcal{V}^2=1$. The marginal probability density $|\alpha_i|^2$ (blue) peaks where the visibility is lowest, thus making the maximum visibility $\mathcal{V}_{\max}$ significantly higher than the average visibility. Further, the predictability is clearly enhanced by the use of an HG_{01} pump mode (*B*) compared with the case of an HG_{00} pump mode (*A*). We modified the scale of $|\alpha_i|^2(p_{s,x})$ to fit the probability density on the same graph as the two other curves.

this unavoidably leads to a mixed-state density matrix. This implies that there can be no such entanglement if the measurement shows the subsystem to be in a pure quantum state. Within this constraint, the measurements on the subsystem and on the remaining part can of course be correlated, but this information is not accessible by looking at only one subsystem. This is essentially the message of the no-signaling theorem (17): It is impossible to detect whether a measurement has been performed on one of two entangled subsystems by looking exclusively at the other subsystem. All experiments so far comply with this interpretation. Nevertheless it is important to check such predictions again and again when novel experimental techniques become available.

Conclusions

We have derived the tightest possible relation, Eq. **3**, between the average predictability and the average visibility of a two-alternative system in the presence of an environment. This duality relation proved useful in the analysis of an apparent violation of the duality principle. The selection of one particular subset of the environment and a high degree of nonseparability between the main system and the environment are key to understanding this apparent violation. According to our analysis, the duality principle in its standard form is safe and sound, but our duality relation remains to be thoroughly tested.

Materials and Methods

Details of the Model of the Two-Photon Experiment. We start by using the known theory of SPDC, which provides an analytic solution for the two-photon mode function in wavevector space $\Psi(\mathbf{p_s}, \mathbf{p_i})$, to compute the mode function $\Psi(\mathbf{r_s}, \mathbf{r_i})$ in the image plane of the source (18–22). We describe our approach to computing $\Psi(\mathbf{r_s}, \mathbf{r_i})$ in the first section of *SI Text*.

In our model, we use a two-slit mask with a slit separation d in the image plane of the output facet of the crystal on the signal photon side. Upon measurement of the idler photon position, the correlations allow one to gain knowledge about which slit the signal photon traverses while measuring the interference pattern in the far field of the two-slit mask. We model the mask with the transmission function $W(r_{s,y}) = T(r_{s,y}) + B(r_{s,y})$, where T and B stand for the "top" and "bottom" slits and correspond to rectangle functions of width Δ at positions $d/2$ and $-d/2$, respectively. We chose the letter W for the two-slit mask because it looks like what it represents: two slits with light diffracting out. The unnormalized two-photon mode function after one of the three masks is given by $\Psi_S(\mathbf{r_s}, \mathbf{r_i}) = \Psi(\mathbf{r_s}, \mathbf{r_i})S(r_{s,y})$, where S can be replaced by W, T, or B. The single-slit amplitudes $\Psi_T(\mathbf{r_s}, \mathbf{r_i})$ and $\Psi_B(\mathbf{r_s}, \mathbf{r_i})$ are needed in the thorough analysis of the test of the duality principle and are physically obtainable by blocking the bottom slit or the top slit, respectively. As we are interested in the joint probability of the signal photon being detected in the far field of the mask and the idler photon in the near field of the crystal, we perform a Fourier transform on the signal photon only: $\tilde{\Psi}_S(\mathbf{p_s}, \mathbf{r_i}) = (2\pi)^{-1}\int d\mathbf{r}\ \Psi_S(\mathbf{r}, \mathbf{r_i})e^{i\mathbf{r}\cdot\mathbf{p_s}}$.

The idler photon is detected with a multimode fiber (MMF) of width w_f at position ($r_{i,x} = 0$, $r_{i,y} = d/2$). The mode of this fiber is modeled by a Gaussian function:

$$f(\mathbf{r_i}) = \exp\left\{\frac{-\left[r_{i,x}^2 + (r_{i,y} - d/2)^2\right]}{(2w_f^2)}\right\}. \quad [4]$$

Upon detection of an idler photon, the conditional distributions of the signal photon in coordinate space and wavevector space are respectively written

$$P_S(\mathbf{r_s}|f_i) = N_P \int d\mathbf{r_i}|\Psi_S(\mathbf{r_s}, \mathbf{r_i})f_i(\mathbf{r_i})|^2 \quad [5]$$

and

$$\tilde{P}_S(\mathbf{p_s}|f_i) = N_P \int d\mathbf{r_i}|\tilde{\Psi}_S(\mathbf{p_s}, \mathbf{r_i})f_i(\mathbf{r_i})|^2, \quad [6]$$

where the normalization constant is given by

$$N_P^{-1} = \iint d\mathbf{r_s}d\mathbf{r_i}|\Psi_W(\mathbf{r_s}, \mathbf{r_i})f_i(\mathbf{r_i})|^2. \quad [7]$$

We find Eqs. **5** and **6** through conditional probabilities. For instance, in the near field of the two-slit mask, the conditioned signal photon distribution is given by $P_S(\mathbf{r_s}|f_i) = P_S(\mathbf{r_s}, f_i)/P_S(f_i)$, where $P_S(f_i) = N_P^{-1}$ and $P_S(\mathbf{r_s}, f_i)$ is equal to the remaining integral in Eq. **5**.

In view of the duality relations, the probability distribution $\tilde{P}_W(\mathbf{p_s}|f_i)$ is composed of one main degree of freedom and one that belongs to the environment: the vertical and horizontal directions, respectively. In general, the visibility of the interference pattern depends on the degree of freedom of the environment and can thus vary as a function of $p_{s,x}$.

We chose to calculate the average predictability in wavevector space, which allows us to retrieve the which-alternative knowledge in the same basis as the visibility. We retrieve $\tilde{P}_T(\mathbf{p_s}|f_i)$ and $\tilde{P}_B(\mathbf{p_s}|f_i)$ by blocking slit *B* or slit *T*, respectively. We then integrate the distributions in wavevector space over the main degree of freedom, p_y, and obtain the marginal probability distributions $|\alpha|_T^2(p_{s,x}) = \int dp_{s,y}\tilde{P}_T(p_{s,x}, p_{s,y}|f_i)$ and $|\alpha|_B^2(p_{s,x}) = \int dp_{s,y}\tilde{P}_B(p_{s,x}, p_{s,y}|f_i)$. For brevity, we henceforth omit writing the argument $p_{s,x}$. The marginal signal probability distribution for the two slits simultaneously in the same basis is $|\alpha|_W^2 = |\alpha|_T^2 + |\alpha|_B^2$; note that $|\alpha|_W^2$ is denoted $|\alpha_i|^2$ in the main text. Predictability and visibility can both be expressed as a function of $p_{s,x}$: $\mathcal{P} = \left||\alpha|_T^2 - |\alpha|_B^2\right|/|\alpha|_W^2$ and $\mathcal{V} = 2|\alpha_T\alpha_B|/|\alpha|_W^2$. The average predictability and average visibility are respectively given by

$$\overline{\mathcal{P}} = \int dp_{s,x}\left||\alpha|_T^2 - |\alpha|_B^2\right| \quad [8]$$

and

$$\overline{\mathcal{V}} = \int dp_{s,x}2|\alpha_T\alpha_B|. \quad [9]$$

Interestingly, in all of the particular cases that we consider, the quantity $|\alpha|_T^2 - |\alpha|_B^2$ is always positive because it is always more probable that two photons of a pair go through the same slit rather than opposite slits. Consequently, the average predictability measured without sorting the states of the environment,

as in refs. 10 and 11, is identical to the average predictability measured after sorting the states of the environment, as in the calculation presented here.

The last quantities left to find are the following variances:

$$\sigma_{\mathcal{P}}^2 = \int dp_{s,x} |\alpha|_W^2 \left(\mathcal{P} - \overline{\mathcal{P}}\right)^2 \quad [10]$$

and

$$\sigma_{\mathcal{V}}^2 = \int dp_{s,x} |\alpha|_W^2 \left(\mathcal{V} - \overline{\mathcal{V}}\right)^2. \quad [11]$$

Using Eqs. **4**–**11** and the SPDC mode function, we check that Eq. **3** is satisfied by means of a numerical example. In our model, the pump spatial transverse mode does not play a key role and need not be of any special kind. We thus consider a plane wave, which is a very good approximation to a collimated Gaussian beam at the crystal in that the differences in the results are negligible. For the numerical calculations, the set of parameters that we use is $\{\varphi = -19$ rad, $L = 2$ mm, $d = 70$ μm, $\Delta = d/4$ μm, $w_f = 10$ μm, $n = 1.65$, $\lambda_p = 405$ nm$\}$, where L is the crystal length, n is the crystal average index, and λ_p is the wavelength of the pump in vacuum.

ACKNOWLEDGMENTS. The authors thank Ralf Menzel and Wolfgang Schleich for useful discussions regarding the interpretation of their experiment. This work was supported by the Canada Excellence Research Chairs Program. E.B. acknowledges the financial support of the Fonds de recherche Nature et technologies, Grants 149713 and 176729.

1. Bohr N (1951) *Albert Einstein: Philosopher-Scientist, Discussion with Einstein on Epistemological Problems in Atomic Physics*, ed Schilpp PA (Northwestern University and Southern Illinois University, Open Court, Evanston, IL).
2. Wootters WK, Zurek WH (1979) Complementarity in the double-slit experiment: Quantum nonseparability and a quantitative statement of Bohr's principle. *Phys Rev D Part Fields* 19(2):473.
3. Greenberger DM, Yasin A (1988) Simultaneous wave and particle knowledge in a neutron interferometer. *Phys Lett A* 128(8):391–394.
4. Scully MO, Englert B-G, Walther H (1991) Quantum optical tests of complementarity. *Nature* 351:111–116.
5. Jaeger G, Shimony A, Vaidman L (1995) Two interferometric complementarities. *Phys Rev A* 51(1):54–67.
6. Englert BG (1996) Fringe visibility and which-way information: An inequality. *Phys Rev Lett* 77(11):2154–2157.
7. Englert B-G, Bergou JA (2000) Quantitative quantum erasure. *Opt Commun* 179(1): 337–355.
8. Schwindt PDD, Kwiat PG, Englert B-G (1999) Quantitative wave-particle duality and nonerasing quantum erasure. *Phys Rev A* 60(6):4285.
9. Dürr S, Nonn T, Rempe G (1998) Fringe visibility and which-way information in an atom interferometer. *Phys Rev Lett* 81(26):5705.
10. Menzel R, Puhlmann D, Heuer A, Schleich WP (2012) Wave-particle dualism and complementarity unraveled by a different mode. *Proc Natl Acad Sci USA* 109(24): 9314–9319.
11. Menzel R, et al. (2013) A two-photon double-slit experiment. *J Mod Opt* 60(1):86–94.
12. Rowe MA, et al. (2001) Experimental violation of a Bell's inequality with efficient detection. *Nature* 409(6822):791–794.
13. Adenier G, Khrennikov AY (2007) Is the fair sampling assumption supported by EPR experiments? *J Phys At Mol Opt Phys* 40(1):131.
14. Giustina M, et al. (2013) Bell violation using entangled photons without the fair-sampling assumption. *Nature* 497(7448):227–230.
15. Spreeuw RJC (1998) A classical analogy of entanglement. *Found Phys* 28(3):361–374.
16. Borges CVS, Hor-Meyll M, Huguenin JAO, Khoury AZ (2010) Bell-like inequality for the spin-orbit separability of a laser beam. *Phys Rev A* 82(3):033833.
17. Ghirardi GC, Rimini A, Weber T (1980) A general argument against superluminal transmission through the quantum mechanical measurement process. *Lett Nuovo Cimento* 27(10):293–298.
18. Monken CH, Souto Ribeiro PH, Pádua S (1998) Transfer of angular spectrum and image formation in spontaneous parametric down-conversion. *Phys Rev A* 57(4):3123.
19. Pires HDL, van Exter MP (2009) Near-field correlations in the two-photon field. *Phys Rev A* 80(5):053820.
20. Peeters WH, Renema JJ, van Exter MP (2009) Engineering of two-photon spatial quantum correlations behind a double slit. *Phys Rev A* 79(4):043817.
21. Chan KW, Torres JP, Eberly JH (2007) Transverse entanglement migration in hilbert space. *Phys Rev A* 75(5):050101.
22. Pires HDL, van Exter MP (2009) Observation of near-field correlations in spontaneous parametric down-conversion. *Phys Rev A* 79(4):041801.